

## Nonthermal Power Law Decay of Metal Dimer Anions

J. Fedor,<sup>1</sup> K. Hansen,<sup>2</sup> J. U. Andersen,<sup>3</sup> and P. Hvelplund<sup>3</sup>

<sup>1</sup>*Institute for Ion Physics, Technikerstrasse 25, Leopold-Franzens Universität, A-6020 Innsbruck, Austria*

<sup>2</sup>*Department of Physics, Gothenburg University, SE-41296 Gothenburg, Sweden*

<sup>3</sup>*Department of Physics and Astronomy, University of Aarhus, DK-8000 Aarhus C, Denmark*

(Received 6 October 2004; published 23 March 2005)

The metastable decay of dimer anions of Cu and Ag has been measured in a storage ring. The decay is found to proceed nonexponentially and is well described by a power law with an exponent of  $-1$ . This signals the presence of a continuum of decay constants in the ensemble. This quasicontinuum can be provided by the quantum mechanical tunneling decay of high angular momentum states populated in the source. Numerical calculations for dimers of a variety of elements suggest that this decay behavior can be expected for a wide range of species.

DOI: 10.1103/PhysRevLett.94.113201

PACS numbers: 34.10.+x, 33.15.Mt, 36.40.Qv

Common phenomena in molecular beam experiments involving clusters and molecules are unimolecular reactions, in which atoms, small molecules, or electrons are emitted thermally. These decays have been successfully described with statistical theories: an excitation energy in the continuum randomizes, and emission of an atom or a group of atoms results from accidental concentration of sufficient energy on these few degrees of freedom. Such thermal statistical decays are limited to systems where some degree of randomization is possible. For molecules and clusters, where the approximately harmonic vibrations of the nuclei are by far the dominant contribution to the heat capacity, this requires at least two vibrational degrees of freedom, and diatomic molecules are therefore not expected to show a thermally induced metastable decay.

In this Letter we report on the observation of unimolecular decay of  $\text{Cu}_2^-$  and  $\text{Ag}_2^-$  on time scales from tens of microseconds to tens of milliseconds. The dimer anions were produced in a Cs sputter source [1], along with a number of anionic clusters of the same materials and some Cs alloyed particles. The source has previously been used to produce small anionic clusters, and is known to produce clusters with energies in the continuum [2]. The ions were accelerated to 22 keV and mass selected with a  $90^\circ$  magnetic deflection. The mass resolution of the magnet was sufficient to discriminate the small amount of hydrogen contaminated dimers from the pure dimers. For both copper and silver, only the lowest mass combination of the two isotopes was used in the experiments. The magnet only selects a mass-to-charge ratio, but the isotope distribution ruled out any significant amount of doubly charged tetramers in the beam. After acceleration and mass selection, the beam was injected into a small electrostatic storage ring, ELISA, with a storage time of several seconds, mainly limited by collisions with the residual gas [3]. The circulation period in the 6.3 m circumference ring is several tens of microseconds. The decay is measured when the anions pass through a ca. 1 m long linear piece of the ring. The neutral products continue straight through the

bending electrode and hit a multichannel plate detector. The signal measured is thus proportional to the decay rate and not to the remaining population.

The measured curves for both species are shown in Fig. 1, where  $1/\text{counts}$  is plotted versus the time after injection. Over a large range the curves are well represented by straight lines which implies a temporal decay of the  $1/t$  type. At long times the signal curves downwards. This is caused by a contribution to the decay from collisions with the residual gas.

These results are very similar to previous experiments on metal clusters with the same equipment [2], as well as experiments on fullerenes [4] and on biomolecules [5] with other sources. The power law decay observed in these experiments can be explained by the presence of a broad continuum of thermal decay constants in the ensemble produced in the source. It is expected to be a general feature of isolated, energetically disperse ensembles of clusters and molecules.

A similar continuum of thermal rate constants does not exist for a single vibrational degree of freedom. On the other hand, the manifestation of  $1/t$  decay hinges only on the presence of a sufficiently broad and dense set of rate constants, populated with similar amplitudes. We conclude that the dimer decay observed here must be nonthermal, but still with a broad continuum of decay constants.

From the limited number of possible origins for the delayed dissociation of diatomic molecules [6], the presence of a metastable electronic state decaying either through emission of radiation [7] or electronic predissociation [8] is unlikely to lead to decays over such a wide range of experimental times. On purely energetic grounds it is not possible to rule out decay by electron emission, but for a range of states this channel is eliminated by angular momentum conservation. The highest angular momentum carried away by an emitted electron with a certain kinetic energy can be estimated either from the Langevin capture cross section or from the geometric size of the molecule. Both are weakly increasing functions of the energy, and for

1 eV the values are of order unity. This should be compared with typical  $L$  values of several hundred (see below). Thus the rotational energy is effectively tied up and only the vibrational energy needs to be considered in the decay.

At sufficiently high angular momentum, the barrier is high enough to accommodate one or usually more quasibound vibrational states in the continuum. Figure 2 illustrates this. The  $\text{Cu}_2^-$  ground state potential is adopted from [9] and for finite rotational quantum number  $L$  modified by the angular momentum barrier,  $\hbar^2 L(L+1)/2\mu r^2$ , where  $\mu$  is the reduced mass of the dimer and  $r$  the separation between the atoms. In the example shown, 18 quasibound vibrational states are above zero energy (not counting the angular momentum degeneracy) and will decay by tunneling through the effective barrier. Indexing this rate constant by the vibrational and rotational quantum numbers,  $k(v, L)$ , we have the following expression for the measured signal at time  $t$ :

$$I(t) = \sum_{v,L} (2L+1)k(v, L)e^{-k(v,L)t}\rho(v, L) \quad (1)$$

up to a constant which accounts for the detection efficiency. Here  $\rho(v, L)$  is the number of stored molecules with the quantum numbers indicated.

The tunneling decay rate constant,  $k(v, L)$ , is calculated as  $\nu|T|^2$ , where  $|T|^2$  is the tunneling probability, and  $\nu$  is an attempt frequency with which the internuclear separation hits the barrier. We expect this frequency to be similar to the vibrational frequency of the dimer, i.e.,  $\nu_d = 5.63 \times 10^{12}$  Hz for  $\text{Cu}_2^-$  and  $\nu_d = 4.35 \times 10^{12}$  Hz for  $\text{Ag}_2^-$  [9].

The identification of the classical frequency with the quantum mechanical attempt frequency was tested on a harmonic potential. We calculated the flux towards the barrier,  $|\psi(x_t)|^2\langle v_+ \rangle$ , where  $|\psi(x_t)|^2$  is the density at the classical turning point  $x_t$  and  $\langle v_+ \rangle$  is the expectation value of the positive speeds,  $\langle v_+ \rangle = \int_0^\infty |\psi(p)|^2(p/\mu)dp$ , where  $\psi(p)$  is the wave function in momentum space. Given the high vibrational quantum numbers, we can calculate  $\langle v_+ \rangle$  semiclassically with the momentum distribution  $\sqrt{E - p^2/2\mu}$ . This gives  $\langle p_+ \rangle = \sqrt{(2\mu E)}/\pi$  or  $\langle v_+ \rangle = \sqrt{(2E/\mu)}/\pi$ . The density at the classical turning point was calculated with the recurrence relation for Hermite polynomials,  $H_{n+1} - 2xH_n + 2nH_{n-1} = 0$ , where  $x$  is the scaled coordinate [10]. The numerical values of these frequency factors vary smoothly between  $\nu/\nu_d = 0.3$  and  $\nu/\nu_d = 1.8$  for  $v = 2$  to 10 000. Based on this near coincidence of the quantum mechanical and classical attempt frequencies for the harmonic oscillator, we used the corresponding classical attempt frequencies calculated with the more realistic potential, i.e.,  $\nu^{-1} = t_{cl}$ , where  $t_{cl}$  is the classical period in the anharmonic motion.

The positions of the quasibound levels and their tunneling probabilities  $|T|^2$  were calculated numerically. The

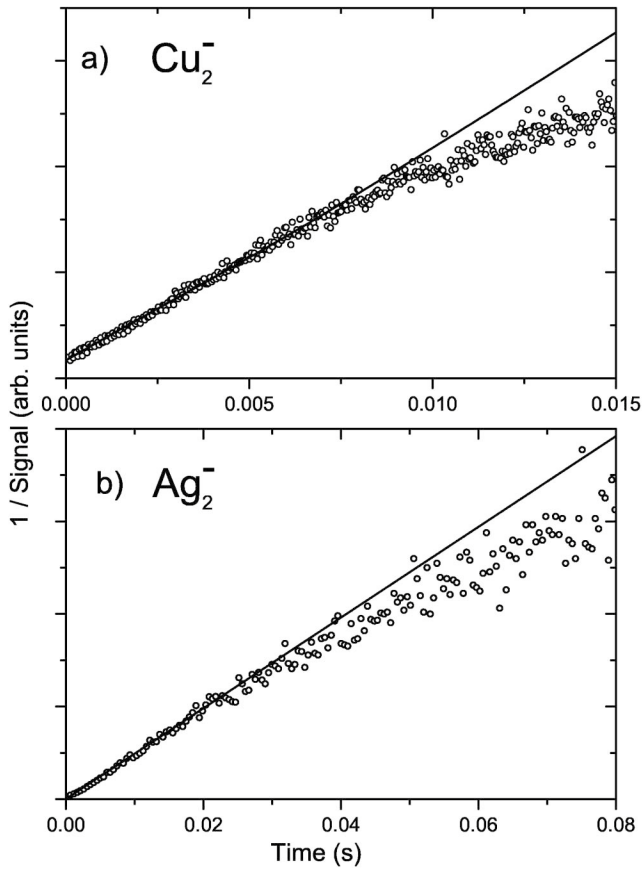


FIG. 1. The time dependence of the reciprocal of the signal in the neutrals detector for (a)  $\text{Cu}_2^-$  and (b)  $\text{Ag}_2^-$ . The counts are bunched into one point for each turn in the storage ring for  $\text{Cu}_2^-$ . For  $\text{Ag}_2^-$  three turns are bunched into one point. The offset in time for Cu is due to the finite time of extraction from the source. Also shown is the time dependence of the decay intensity (solid lines), calculated using Eq. (1) with identical population of all rotational and vibrational states,  $\rho(v, L) = \text{const}$ .

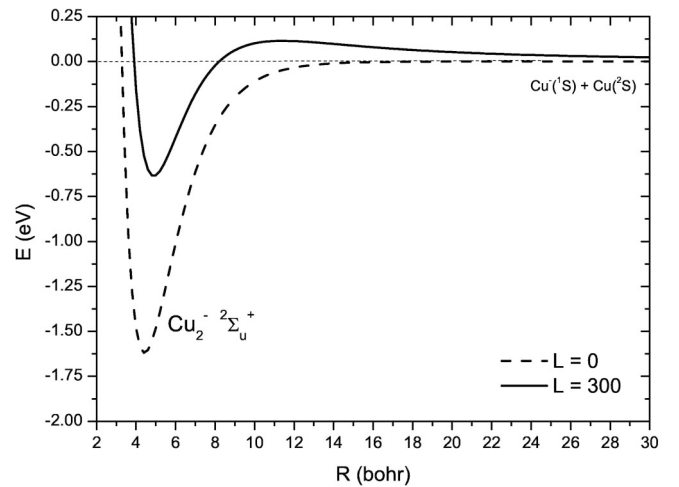


FIG. 2. Potential energy curve of the ground electronic state of  $\text{Cu}_2^-$  [9] (dashed curve). The solid line represents the effective potential at the rotational quantum number  $L = 300$ .

Schrödinger equation for the movement of the nuclei was solved using the Numerov method [11] and the continuum wave functions were normalized to a  $\delta$  function in energy [12]. The phase shift technique [13] was applied to find the positions of the orbiting resonances for each rotational quantum number  $L$ . With the wave function established, the tunneling matrix element squared was calculated with the Wentzel-Brillouin-Kramers (WKB) approximation [14].

$$|T|^2 = \exp\left(-\frac{\sqrt{8\mu}}{\hbar} \int_{R_1}^{R_2} \sqrt{V_{\text{eff}}(L, R) - E} dR\right), \quad (2)$$

where  $R_1$  and  $R_2$  are the classical turning points of the barrier.

The smallest angular momentum that can accommodate a metastable state is  $L = 130$  for  $\text{Cu}_2^-$  and  $L = 250$  for  $\text{Ag}_2^-$ . The states disappear again at  $L = 480$  and  $L = 600$ , where the potential minimum becomes too shallow to accommodate any quasibound state. At the extreme  $L$  values, the lifetimes are only marginally longer than the vibrational period. As the depth of the potential increases, the longest lived states acquire lifetimes that grow exponentially and reach values up to  $10^{250}$  s. Experimental time scales are thus well within the extremes of this distribution of rate constants. Figure 3 samples a range of calculated lifetimes of the  $\text{Cu}_2^-$  quasibound levels. The large number of states effectively forms a continuum and we can approximate the experimental signal in Eq. (1) with an integral. The variation of the rate constant is to a very high degree determined by the matrix element, which depends exponentially on the barrier. We therefore assume a broad

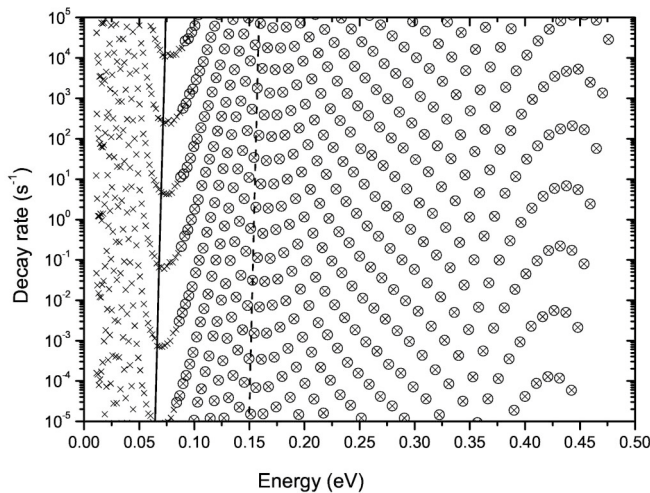


FIG. 3. Positions and lifetimes of the quasibound levels of  $\text{Cu}_2^-$ . Only a representative range of lifetimes is shown. For illustration we have connected resonances with the vibrational quantum number  $\nu = 80$  and varying angular momentum (solid line), and resonances with  $L = 340$  (dashed line). The states with vibrational energy less than the electron affinity of  $\text{Cu}_2$  are indicated by open circles-crosses.

distribution of the argument in the WKB expression. Substituting  $k = \nu|T|^2$  and  $x \equiv -\ln(|T|^2)$  the intensity integral reads

$$I(t) \propto \int_0^\infty \nu \exp(-x) e^{-\nu \exp(-x)t} dx. \quad (3)$$

This furthermore assumes that the population of decaying states, as produced in the source, is reasonably smooth. The angular momentum degeneracy has been included into the proportionality sign. The justification for this is that the lifetime is virtually uncorrelated with  $L$  in the relevant time range. The density of states versus  $\ln(|T|^2)$  is shown in Fig. 4. The  $L$  degeneracy is included in the plot. The analogous figure without this degeneracy is qualitatively similar. The integral in Eq. (3) is easily calculated:

$$I(t) \propto \frac{1}{t} (1 - e^{-\nu t}) \approx \frac{1}{t}. \quad (4)$$

The approximations used can be checked by numerical evaluation of Eq. (1). Figure 1 includes the decays calculated with the full expression. As expected, the deviation from the straight line of Eq. (4) is very minor.

The source is not thermal, and the determination of the distribution of excitation energies is a nontrivial task. The vibrational energies involved must be on the order of the dissociation energies, i.e., 1.62 eV and 1.37 eV [9] for  $\text{Cu}_2^-$  and  $\text{Ag}_2^-$ , respectively. The rotational energies span a factor of about 10 for both species, with typical values of a few hundred meV. Although these values are high compared to usual thermal energies, they are still only a fraction of the cohesive energy per atom of the surfaces from which the dimers originate, and considering the strong element of nonthermal processes involved in the sputtering

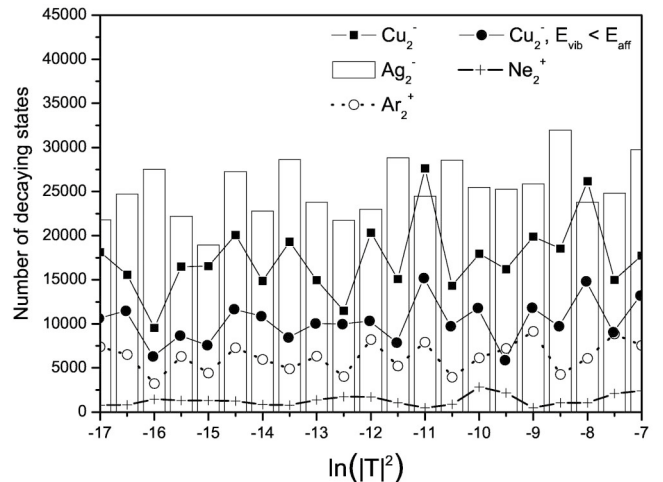


FIG. 4. The  $\ln(|T|^2)$  distribution of calculated decaying states, the width of the histogram bars is 0.5. The  $x$ -axis range corresponds to the range of  $\text{Cu}_2^-$  lifetimes of Fig. 3. The angular momentum degeneracy of  $2L + 1$  is included in the count. Also shown is the statistics for states with vibrational energy less than the electron affinity of  $\text{Cu}_2$ .

process, they do not seem unrealistic. Indeed, measurements of the kinetic energy distributions of neutral silver atoms show broad distributions peaked at energies around 1 eV [15]. Similar results for Ni and Co show that this is not specific to silver [16]

The numerical calculations for  $\text{Ag}_2^-$  using the Morse potential from [9] with the *ab-initio*  $R_e$  value from [17] yield basically the same results as those for  $\text{Cu}_2^-$ , viz., a high number of decaying states and a  $1/t$  intensity dependence in accord with the experimental findings. One difference between Cu and Ag is the significantly different time scale on which the collisional decay induced by the rest gas in the ring becomes important. One possible explanation for this could be a difference in the number of decaying states, which is proportional to the densities in Fig. 4, relative to the number of bound vibrational states. A comparison of these two numbers does not support the suggestion. An alternative explanation may be based on the collision dynamics. The c.m. collision energy is less for Ag than for Cu, and at the same time both the atomic binding energy for  $\text{Ag}_2^-$  and the electron affinity of  $\text{Ag}_2$  are higher. These differences may cause a reduced destruction cross section for the  $\text{Ag}_2^-$  compared with that of  $\text{Cu}_2^-$ , effectively delaying the onset of collisional decay of the former.

Expressions (3) and (4) suggest that the  $1/t$  decay law is a general feature, subject mainly to limitations in the preparation of the highly excited states. Motivated by this suggestion, we repeated the numerical calculation of the positions and rates of the decaying rotational states for several dimers. As a representative set, rare gas dimer cations  $\text{Ne}_2^+$ ,  $\text{Ar}_2^+$ ,  $\text{Kr}_2^+$ , and  $\text{Xe}_2^+$  with *ab-initio* ground state potentials from [18,19], were chosen. The quasibound state energy versus lifetime map is sufficiently dense in most cases, and has an almost constant distribution of  $\ln(\nu|T|^2)$ , modulo statistical fluctuations, although a weak increase may be present (see Fig. 4). The only visible deviation from a straight line on a  $1/\text{counts}$  plot occurs for  $\text{Ne}_2^+$ . Everything else being equal, the number of decaying states decreases with decreasing reduced mass of the dimer.

In conclusion, we have shown experimentally that ensembles of two different metal dimer ions, produced with high internal excitation energy in a sputter source, decay with a  $1/t$  rate. The observations can be explained as the tunneling decay of highly rotationally and vibrationally excited molecules. The metastable molecules have a highly disperse range of lifetimes, covering more than 200 orders of magnitude, and the  $1/t$  behavior is robust towards the precise values of individual lifetimes. Furthermore, the calculations suggest that the  $1/t$  law is to be expected in

most diatomic ions if a broad range of rotational states is populated in experiments.

This work was supported by the Danish National Research Foundation through Aarhus Center for Atomic Physics (ACAP), FWF Wien, the European Union under Contract No. HPRN-CT-2000-00026, and the Swedish National Research Council (VR).

- 
- [1] P. Tykesson, H.H. Andersen, and J. Heinemeier, IEEE Trans. Nucl. Sci. **23**, 1104 (1976).
  - [2] K. Hansen, J.U. Andersen, P. Hvelplund, S.P. Møller, U.V. Pedersen, and V.V. Petrunin, Phys. Rev. Lett. **87**, 123401 (2001).
  - [3] S.P. Møller, Nucl. Instrum. Methods Phys. Res., Sect. A **394**, 281 (1997).
  - [4] J.U. Andersen, C. Gottrup, K. Hansen, P. Hvelplund, and M.O. Larsson, Eur. Phys. J. D **17**, 189 (2001).
  - [5] J.U. Andersen, H. Cederquist, J.S. Forster, B.A. Huber, P. Hvelplund, J. Jensen, B. Liu, B. Manil, L. Maunoury, S.B. Nielsen, U.V. Pedersen, H.T. Schmidt, S. Tomita, and H. Zettergren, Eur. Phys. J. D **25**, 139 (2003).
  - [6] J.M. Brown and A. Carrington, *Rotational Spectroscopy of Diatomic Molecules* (Cambridge University Press, Cambridge, England, 2003).
  - [7] J. Fedor, K. Gluch, R. Parajuli, S. Matt-Leubner, O. Echt, P. Scheier, and T.D. Märk, J. Chem. Phys. **121**, 7253 (2004).
  - [8] J. Fedor, R. Parajuli, S. Matt-Leubner, O. Echt, F. Hagelberg, K. Gluch, A. Stamatovic, M. Probst, P. Scheier, and T.D. Märk, Phys. Rev. Lett. **91**, 133401 (2003).
  - [9] J. Ho, K.M. Erwin, and J.C. Lineberger, J. Chem. Phys. **93**, 6987 (1990).
  - [10] L. Pauling and E.B. Wilson, *Introduction to Quantum Mechanics* (McGraw-Hill, New York, 1935).
  - [11] T. Pang, *Introduction to Computational Physics* (Cambridge University Press, Cambridge, England, 1997).
  - [12] R.J. Le Roy and W.K. Liu, J. Chem. Phys. **69**, 3622 (1978).
  - [13] Z. Chen, I. Ben-Itzhak, C.D. Lin, W. Koch, G. Frenking, I. Gertner, and B. Rosner, Phys. Rev. A **49**, 3472 (1994).
  - [14] J.S. Townsend, *A Modern Approach to Quantum Mechanics* (University Science, Sausalito, California, 2000).
  - [15] W. Berthold and A. Wucher, Phys. Rev. B **56**, 4251 (1997).
  - [16] P. Lievens, V. Philippsen, E. Vandeweert, and R.E. Silverans, Nucl. Instrum. Methods Phys. Res., Sect. B **135**, 471 (1998).
  - [17] V. Bonacic-Koutecky, L. Cespiva, P. Fantucci, J. Pittner, and J. Koutecky, J. Chem. Phys. **100**, 490 (1994).
  - [18] T.K. Ha, R. Rupper, A. Wüest, and F. Merkt, Mol. Phys. **101**, 827 (2003).
  - [19] I. Paidarova and F.X. Gadea, Chem. Phys. **274**, 1 (2001).